Available online at www.sciencedirect.com

SCIENCE DIRECT

European Journal of Pharmacology 505 (2004) 19–29

www.elsevier.com/locate/ejphar

# Basal calcium entry in vascular smooth muscle

Damon Poburko[a,b,c,*], Philippe Lhote[a], Tania Szado[b,c], Tasneim Behra[c], Roshanak Rahimian[d], Bruce McManus[c], Cornelis van Breemen[b,c,1], Urs T. Ruegg[a,1]

[a]Group of Pharmacology, School of Pharmacy, Universities of Geneva and Lausanne, 1015 Lausanne, Switzerland
[b]Department of Pharmacology and Therapeutics, University of British Columbia, Vancouver, Canada V6T 1Z3
[c]The James Hogg iCAPTUR[4]E Centre, St. Paul's Hospital/Providence Health Care, University of British Columbia, Vancouver, Canada V6Z 1Y6
[d]Thomas J. Long School of Pharmacy and Health Sciences, University of the Pacific, Stockton, CA 95211, USA

Received 22 September 2004; accepted 28 September 2004

**Abstract**

Basal calcium leak into smooth muscle was identified 30 years ago yet remains poorly understood. We characterized this leak measuring $^{45}Ca^{2+}$ uptake into cultured rat aortic smooth muscle cells. Wash solution (0 °C) containing lanthanum (3 mM) removed extracellular tracer and increased cellular $^{45}Ca^{2+}$ retention more effectively than EGTA (0.2 mM). Basal $Ca^{2+}$ entry was $1.45\times10^{9}$ $Ca^{2+}\cdot cell^{-1}\cdot min^{-1}$. This translated to ~250 $\mu mol^{-1}\cdot min^{-1}$ given cell volumes of 4–15 pl as determined by 3-D image reconstruction. Gadolinium (100 μM) blocked 80% of the leak and exhibited a biphasic concentration–response relation ($IC_{50}$s=1 μM and 2 mM). Organic ion channel blockers also inhibited ~80% of the leak; 45% by nifedipine (10 μM), 7% was exclusively blocked by SKF 96365 (1-[*b*-[3-(4-Methoxyphenyl)propoxy]-4-methoxyphenethyl]-1H-imidazole) (50 μM) and 23% was exclusively sensitive to 2-aminoethoxydiphenylborate (2-APB, 75 μM). Reverse transcriptase polymerase chain reaction revealed TrpC1, 4 and 6 mRNA, and we propose that 2-APB may selectively block TrpC4-containing channels. We conclude that basal $Ca^{2+}$ entry is mainly due to a basal open probability of excitable $Ca^{2+}$-channels.


*Keywords:* Basal entry; Calcium; Vascular smooth muscle

## 1. Introduction

Described in smooth muscle 30 years ago, the phenomenon of basal calcium entry has received little attention especially in smooth muscle cells, where it plays a substantial role in resting calcium homeostasis and the maintenance of vascular tone (Fayazi et al., 1996; Obejero-Paz et al., 1998; van Breemen et al., 1973). For example exposure of "resting" cells to $Ca^{2+}$ free ambient solution causes a loss of sarcoplasmic reticulum $Ca^{2+}$ content. This is due to leakage of $Ca^{2+}$ from the sarcoplasmic reticulum (Camello et al., 2002), and sarcoplasmic reticulum $Ca^{2+}$ can be restored upon replenishment of $Ca^{2+}$ without the development of force (Casteels and Droogmans, 1981; Deth and van Breemen, 1974). Conversely blockade of $Ca^{2+}$ extrusion in the presence of extracellular $Ca^{2+}$ leads to a net gain in cellular $Ca^{2+}$. Thus it has long been clear that the inactive smooth muscle is not static with respect to $Ca^{2+}$ metabolism, but supports continuous physiological cycling of $Ca^{2+}$ between the intra and extracellular compartments. While it is generally accepted that efflux is mediated by the plasma membrane $Ca^{2+}$-ATPase and the $Na^{+}/Ca^{2+}$-exchanger we have little knowledge to date regarding the mechanisms of resting $Ca^{2+}$ influx (Obejero-Paz et al., 1998; Vandebrouck et al., 2002). The objective of this investigation is therefore to characterize the nature of $Ca^{2+}$ transport across the plasma membrane of non-stimulated smooth muscle cells.

* Corresponding author. Cardiovascular Sciences, Rm. 2099, 950 W. 28th Avenue, Vancouver, BC, Canada V5Z 4H4. Tel.: +1 604 875 3852; fax: +1 604 875 3120.
*E-mail address:* dpoburko@interchange.ubc.ca (D. Poburko).
[1] These authors contributed equally to this article.

0014-2999/$ - see front matter © 2004 Elsevier B.V. All rights reserved.
doi:10.1016/j.ejphar.2004.09.060

Three different techniques are commonly employed for the measurement of cellular $Ca^{2+}$ fluxes: (1) imaging of fluorescent $Ca^{2+}$ indicators, (2) patch clamp electrophysiology and (3) radioactive tracer analysis, each of which has several advantages and disadvantages. While fluorescent $Ca^{2+}$ indicators have allowed us to investigate $Ca^{2+}$ signalling at the subcellular level with high temporal and spatial resolution (Rudolf et al., 2003), this technique is not suited to measurement of resting $Ca^{2+}$ influx because fluorescent measurements do not differentiate between intra and extracellular sources of $Ca^{2+}$. This is a complicating issue since release of intracellular $Ca^{2+}$ stores often activates capacitative calcium entry through store-operated channels. Electrophysiology is an invaluable tool that has provided great insight into the nature of ion channel behaviour. While the technique is capable of detecting tiny single channel currents of spontaneous channel activity, it is unable to detect electro-neutral transport as seen in some ion-exchange mechanisms. Additionally, the leak current associated with the patch seal is difficult to adequately distinguish from resting $Ca^{2+}$ influx. The third method for measuring $Ca^{2+}$ influx is to label the calcium of the bathing solution with $^{45}Ca^{2+}$ and measure the cellular uptake of radioactive label. This method is theoretically the most direct, but is subject to two drawbacks. First, its temporal resolution is relatively poor and therefore sub-optimal for measurement of stimulated $Ca^{2+}$ fluxes. Second, a background signal is generated by non-specific adsorption of $^{45}Ca^{2+}$ to sites within the extracellular space as previously described (Fayazi et al., 1996). Nevertheless we chose this third method as the most likely to provide direct information on the nature of basal $Ca^{2+}$ entry in monolayers of cultured smooth muscle cells, a preparation that lends itself well to removal of extracellular radioactive label. In addition the fact that net non-stimulated $Ca^{2+}$ fluxes have a relatively slow time course reduces the requirement for high temporal resolution in these experiments.

Given that pure lipid bilayers are not inherently leaky to inorganic ions, several mechanisms have been proposed to account for the resting $Ca^{2+}$ permeability of physiological membranes (Busselberg et al., 1994; van Breemen, 1968). The first possibility is that imperfect junctions between phospholipid domains and membrane proteins are permeable to small ions. Second, pinocytosis may bring significant amounts of calcium into the cell, considering the ~10,000-fold difference between extracellular and intracellular $Ca^{2+}$ concentration (Grasso et al., 1992). Third, excitable $Ca^{2+}$-permeable membrane channels may exhibit a degree of basal activity, or flickering, and thereby contribute to basal calcium influx (Nowycky et al., 1985). Our results provide experimental support for the latter hypothesis, and reveal the complexity and importance of the phenomenon of basal calcium entry.

## 2. Methods

### 2.1. Cultures of smooth muscle cells

Rat aortic smooth muscle cells were prepared from aortae of male Wistar Kyoto rats (200–300 g) as previously described (Lo Russo et al., 1996). Cells were cultured in Dulbecco's Modified Eagles Medium supplemented with essential and non-essential amino acids, vitamins, 0.001% ciproxin and 10% fetal calf serum, and kept at 37 °C in a humidified atmosphere of 5% $CO_2$ in air. Cells were seeded at 20,000 cells (between passages 6 and 11) per 16 mm diameter culture well and grown to confluence (ca. 400,000 cells per well) for 7–9 days.

### 2.2. $^{45}Ca^{2+}$ influx measurement

$^{45}Ca^{2+}$ uptake was recorded as previously described with minor modifications (Lo Russo et al., 1996). After two washes in physiological salt solution (physiological saline solution, in mM: NaCl 145, KCl 5, $MgCl_2$ 1, Hepes [4-(2-hydroxyethyl)piperazine-1-ethanesulfonic acid] 5, glucose 10 and $CaCl_2$ 1.2, pH 7.6), the cellular monolayers were pre-incubated at 37 °C for 15 min (20 min when 2-APB (2-aminoethoxy-diphenylborate) was used) in 200 μl physiological saline solution containing the inhibitors. Twenty micro-liters of $^{45}Ca^{2+}$ at 0.02 mCi/ml were added to this solution and cells were incubated for 10 min at 37 °C, or as specifically indicated. Influx was stopped by washing the cells four times at 0.5 min intervals with 0.5 ml of ice-cold 3 mM $LaCl_3$ or 0.2 mM EGTA (ethylene glycol-bis(2-aminoethylether)-*N*,*N*,*N*′,*N*′-tetraacetic acid) in physiological saline solution without calcium, and cells were detached with 50 μl of physiological saline solution containing trypsin (0.25%) and EDTA (ethylenediaminetetraacetic acid, 0.1%) and were lysed with 250 μl of SDS (sodium dodecyl sulfate, 1%). Radioactivity in the lysates was assessed by scintillation counting (Ultima Gold™, Packard, Groningen, NL, and LKB Wallac 1217 Rackbeta™, Turku, Finland). See Appendix A for conversion of cpm to moles of $^{45}Ca^{2+}$.

### 2.3. Curve fitting

#### 2.3.1. Wash out kinetics

Extracellular tracer was removed by sequential washes of the cells at times denoted in Fig. 1. We subtracted the sum of cpm collected in washes previous to each point from the sum of cpm in all washes collected and in the final cell lysate. This treatment depicts the $^{45}Ca^{2+}$ activity present in the wells immediately prior to each wash (Fig. 1). These values were fitted to a single exponential decay using GraphPad Prism 3.0 to determine the rate of tracer removal.

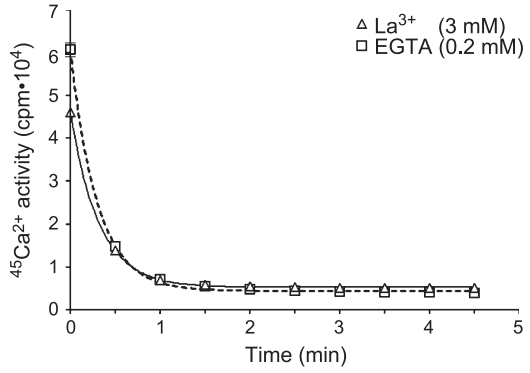


Fig. 1. Optimizing washout of excess tracer. At each time point cells were washed with 0.5 ml ice-cold physiological saline solution containing $LaCl_3$ (3 mM) or EGTA (0.2 mM). $^{45}Ca^{2+}$ activity in the well at each time point was determined by subtracting the sum of $^{45}Ca^{2+}$ activity collected in previous 1 ml washes from the total $^{45}Ca^{2+}$ collected in all washes plus the cell lysate. The $t_0$ point indicates the total $^{45}Ca^{2+}$ activity loaded onto the cells Wash out is best fitted by single exponential decay. Wash out with $LaCl_3$ was described by $k$=3.11±0.08 $min^{-1}$ and plateau=5.28±0.12×$10^3$ cpm · $well^{-1}$. Wash out with EGTA was described by $k$=3.32±0.11 $min^{-1}$ and plateau=4.46±0.22×$10^3$ cpm · $well^{-1}$. Given the equivalent rates of tracer removal using EGTA or $LaCl_3$, $LaCl_3$ was chosen as the superior washing agent in that it resulted in a higher plateau than EGTA.

### 2.3.2. Uptake kinetics

An initial fast component was observed in the raw uptake data. The magnitude of this component was estimated by back extrapolation of the curve to time zero based on the assumption that the rate of uptake would be relatively constant during the first 3 min of influx. Linear regression of these data points (0.5–3.0 min) indicated a $y$-intercept of 96±12 cpm/well. This rapid uptake occurred within the first 30 s of exposure and was subtracted from each data point. The corrected data set was fitted to a single exponential equation using GraphPad Prism 3.0 (Fig. 2).

### 2.3.3. Curve peeling

Visual inspection of the gadolinium ($Gd^{3+}$) concentration–response relationship suggested that $Gd^{3+}$ had a biphasic effect but overlapping concentration–response relationships. GraphPad Prism does not contain an equation to fit such a curve or to estimate the parameters of these two effects ($pIC_{50}$, Hill slope, and magnitude) and to peel the two curves apart. We wrote an equation describing the sum of two sigmoid curves such that the top of the combined curve would be the sum of the two separate curves each with a bottom equal to zero and each with independent $IC_{50}$s and Hill slopes. The equation is shown below:

$$Y = 2 \times \text{Bottom} + \frac{T1 - \text{bottom}}{\left(1 + 10^{((\log IC_{50-1} - X) \times Hill\ Slope1)}\right)} + \frac{(Top - T1 - \text{bottom})}{\left(1 + 10^{((\log IC_{50-1} - X) \times Hill\ Slope2)}\right)}$$

Top−T1 is the top of the second curve. Using GraphPad Prism, the experimental data were fitted to this equation to estimate the individual curve parameters with the initial values set based on visual inspection of the raw data: Bottom=0, T1=70%, Top=100%, $\log(IC_{50\text{-}1})$=−6.0, $\log(IC_{50\text{-}2})$=−3.0, and Hill slope(1and2)=−1.0. The individual curves were then simulated from the best-fit parameters (dotted curves, Fig. 4).

### 2.4. Confocal microscopy and 3-D reconstruction

Cells were transfected with a plasmid encoding a green fluorescent protein (GFP) construct that is targeted to the inner leaf of the plasmalemma with a SNAP-25 presequence (Marsault et al., 1997). Using an Olympus BX50WI microscope fitted with an Ultraview Nipkow confocal disk (Perkin-Elmer, location), z-series of images were captured with a 60× water-dipping lens (numerical aperture 0.90) at 200 nm intervals (Prior H128 motor drive). Image stacks were deconvolved using a Nipkow-optimized classic maximum likelihood estimation algorithm (Huygens, Scientific Volume Imaging, Netherlands). We then reconstructed the image stacks into three-dimensional volumes with Imaris 3.3 (Bitplane, Zurich, Switzerland) and estimated cell volume with the Surpass function using a voxel size of 0.24×0.24×0.20 μm (Fig. 3b).

### 2.5. RNA extraction

Total cellular RNA from low- and high-confluent rat aortic smooth muscle cell lysates were extracted using a RNeasy mini kit™ (Quiagen) according to manufacturer's instructions. RNA was quantified by measuring absorbance spectrophotometrically at 260 nm, and its integrity was

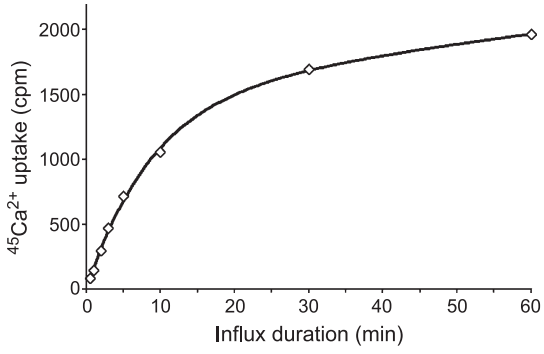


Fig. 2. Exponential $^{45}Ca^{2+}$ uptake. Cells were exposed to $^{45}Ca^{2+}$ (0.6 μCi, 0.9 μM) in the presence of 1.2 mM $^{40}Ca^{2+}$ for the indicated times, and excess tracer was removed with four 30-s washes in ice-cold $LaCl_3$ (3 mM). Linear back extrapolation of the first four points to $t$=0 revealed a $y$-intercept of 96±12 cpm · $well^{-1}$ indicating an initial fast component of tracer uptake that was interpreted as extracellular binding (see Discussion). Following subtraction of this fast component, data were well described by a single exponential process with a plateau of 1.92×$10^3$±0.04×$10^3$ cpm · $well^{-1}$ and a rate constant of 0.084±0.005. Data points represent the mean±S.E. ($n$=6).

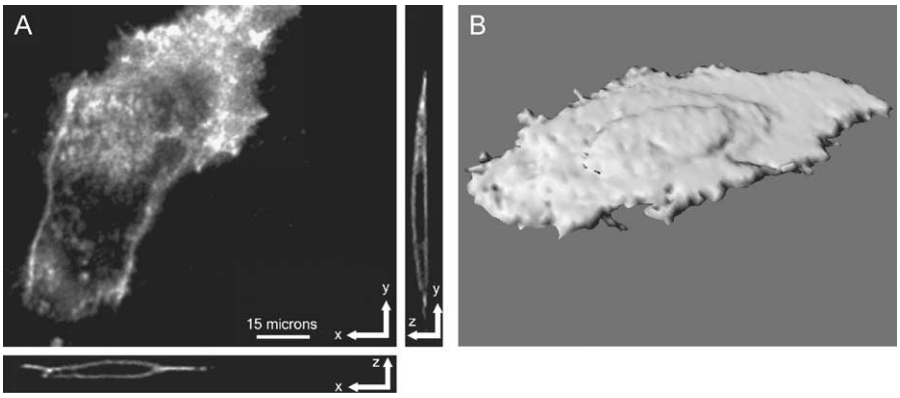


Fig. 3. SNAP-GFP expression pattern and 3-D reconstruction of a representative cell. (A) The peripheral localization of SNAP-GFP is evident in a single image in the $x$–$y$ plane (bird's eye) of a single rat aortic smooth muscle cell amongst a confluent lawn. This localization is also revealed in slices through the $z$–$x$ and $z$–$y$ planes that were produced from deconvolved $z$-stacks using Imaris 3.3 software (Bitplane, Zurich, Switzerland). Scale bar equals 15 μM. (B) These image stacks were then reconstructed into fractal-based volumes using the Surpas feature of Imaris to approximate cell volume (voxel size of $0.24(x)\times0.24(y)\times0.2(z)$ μm), in this case 9 pl.

assessed after electrophoresis in non-denaturating 1% agarose gels stained with ethidium bromide.

### 2.6. Semi-quantitative RT-PCR

Reverse transcription of 5 μg total RNA was performed in 60 μl reaction volumes containing 200 units of Superscript II™ reverse transcriptase, 60 units RNase inhibitor, 3 mM $MgCl_2$, 1×Buffer II (Sigma) and 0.3 μg of random primers and 1 mM dNTP for 50 min at 42 °C. Contaminating genomic DNA present in the RNA preparations was removed by digesting the reaction with 5 units of DNase I for 45 min at 37 °C prior to the addition of reverse transcriptase. RT product (5 μl) was used in each 100 μl PCR reaction. The PCR mixture contained 250 μM dNTP, 2 mM $MgCl_2$, 1×volume of Buffer and 2.5 units Hotstar™ Taq polymerase, and 1 μl of forward and 1 μl of reverse primers. Amplification consisted of 40 cycles of 1 min at 94 °C, 1 min at 55 °C and 1 min at 72 °C. The final extension was completed at 72 °C for 7 min. Ten μl of 6× loading buffer (containing 0.25% bromothymol blue, 0.25% xylene cyanol FF, and 15% Ficoll type 400 (Pharmacia) in distilled water treated with DEPC (diethyl pyrocarbonate)) was added to the PCR products. Twenty μl of PCR products were then analyzed by electrophoresis on 2% agarose gels stained with ethidium bromide and gels were photographed under ultraviolet light. 18S ribosomal RNA expression was used as an internal control. The exemplary gels shown in this report (Fig. 6) represent findings from a minimum of six different low confluency and four high confluency lysates. Rat brain mRNA was used as a positive control for the expression of TrpC1, 2, 3, 4, 5, 6, 7. Primers used for different amplifications were designed from published reports (McDaniel et al., 2001;Walker et al., 2001) or sequences available in Genebank (Table 1). RT-PCR (reverse transcriptase polymerase chain reaction) reactions run in the absence of reverse transcriptase or cDNA were used as negative controls (data not shown). Amplified PCR products from cell lysates were isolated from agarose gel, sequenced and found to be 100% identical to the authentic sequences of rat TrpC1-7.

Table 1
Oligonucleotide sequences of RT-PCR primers

| Channel | GenBank accession no. | Predicted size, bp | Sense/antisense | Location, nucleotides |
|---|---|---|---|---|
| mTrpc1 | U40980 | 372 | 5′-CAAGATTTTGGGAAATTTCTGG-3′ | 1–22 |
| | | | 5′-TTTATCCTCATGATTTGCTAT-3′ | 352–372 |
| rTrpc2 | AF136401 | 487 | 5′-CAGTTTCACCCGATTGGCGTAT-3′ | 1606–1627 |
| | | | 5′-CTTTGGGGATGGCAGGATGTTA-3′ | 2071–2092 |
| hTrpc3 | U47050 | 331 | 5′-ATTATGGTGTGGGTTCTTGG-3′ | 1483–1502 |
| | | | 5′-GAGAAGCTGAGCACAACAGC-3′ | 1795–1814 |
| mTrpc4 | U50922 | 265 | 5′-CAAGGACAAGAGAAAGAAT-3′ | 2535–2553 |
| | | | 5′-CCTGTTGACGAGTAATTTCT-3′ | 2781–2800 |
| mTrpc5 | AF029983 | 419 | 5′-CCTCGCTCATTGCCTTATCA-3′ | 675–694 |
| | | | 5′-TGGACAGCATAGGAAACAGG -3′ | 1075–1094 |
| mTrpc6 | U49069 | 410 | 5′-CTGCTACTCAAGAAGGAAAAC-3′ | 738–758 |
| | | | 5′-TTGCAGAAGTAATCATGAGGC-3′ | 1128–1148 |
| mTrpc7 | AF139923 | 260 | 5′-TGACAGCCAATAGCACCTTCA-3′ | 2397–2417 |
| | | | 5′-GCAGGTGGTCTTTGTTCAGAT-3′ | 2637–2657 |

Trpc, transient receptor potential; m, mouse; r, rat; h, human.

### 2.7. Data analysis

Results are presented as the means of at least three independent experiments with vertical bars indicating standard error (S.E.). $IC_{50}$ values were calculated by non-linear regression using GraphPad Prism 3.0 (GraphPad Software, San Diego, USA). Statistical evaluation was performed using one-way analysis of variance (ANOVA) followed by Bonferroni or Dunnett post-tests. Differences with a value of $P<0.05$ were considered significant.

### 2.8. Materials

Unless specified otherwise drugs and chemicals were purchased from Sigma Aldrich, Switzerland. 2-APB was purchased from Fluka, Switzerland. Ultima Gold™ scintillation cocktail was purchased from Packard, and isotopic $^{45}Ca^{2+}$ was purchased from NEN Life Sciences Products, Geneva. SuperscriptII™ reverse transcriptase, RNase inhibitor and random primers were obtained from Gibco/BRL, Canada. Buffer II (10×) was obtained from Sigma/Aldrich, Canada. $MgCl_2$, dNTP, 10× volume PCR Buffer, Hotstar™ Taq polymerase and RNeasy mini kit™ were purchased from Qiagen, Canada. Primers for ribosomal RNA (18S) and RNAseZap were purchased from Ambion, TX, USA.

## 3. Results

### 3.1. Washout of extracellularly bound tracer $Ca^{2+}$

Fig. 1 illustrates the process of washing out the surface bound $^{45}Ca^{2+}$ from the culture wells as described in the methods. The $^{45}Ca^{2+}$ content of the cellular monolayer falls initially very rapidly when exposed to ice cold solutions containing either $La^{3+}$ (3 mM) or EGTA (0.2 mM) and then stabilizes with a very slow decay. It appeared that the displacement of $^{45}Ca^{2+}$ by $La^{3+}$ ($k$=3.113±0.077) was not appreciably faster than chelation by EGTA ($k$=3.323±0.112). However, it is known that high concentrations of $La^{3+}$ block $Ca^{2+}$ extrusion (Van Breemen and van Breemen, 1969), and this is most probably the reason for the significantly higher plateau following $La^{3+}$ washes ($5.28\times10^3\pm0.12\times10^3$ cpm·well$^{-1}$) than when cells were washed with EGTA ($4.46\times10^3\pm0.22\times10^3$ cpm·well$^{-1}$). On the basis of these results we subsequently use two minutes of washing with ice-cold $La^{3+}$ solution to remove $^{45}Ca^{2+}$ from the wells and outer cell surfaces, thereby permitting the determination of $^{45}Ca^{2+}$ uptake into the cells.

### 3.2. Rate of basal $Ca^{2+}$ influx

The smooth muscle cells were exposed to $^{45}Ca^{2+}$-labelled physiological saline solution ($3.9\times10^4$ cpm·well$^{-1}$ in 0.22 ml) for various times before washout of the surface bound label followed by scintillation counting of cell lysates. Close inspection of the curve revealed an initial very fast component of 96±12 cpm·well$^{-1}$ that was determined by back extrapolation of the linear portion of the curve. This was followed by a mono-exponential component reaching a steady state of $1.92\times10^3\pm0.04\times10^3$ cpm·well$^{-1}$ after about 60 min (see Methods). The size of the initial fast component increased considerably when the time period of the cold $La^{3+}$ was decreased to 30 s (data not shown). This strongly indicated that the fast phase was due to extracellular binding of tracer, so it was subtracted from the curve. The corrected uptake of $^{45}Ca^{2+}$ into the cells (Fig. 2) is best fitted to a single exponential process with a rate constant of 0.084±0.005 cpm·min$^{-1}$. This suggests that, at rest, permeation through the plasma membrane is rate limiting. For the purpose of obtaining highly reproducible measurements of resting $Ca^{2+}$ influx in the presence of a variety of $Ca^{2+}$ transport inhibitors we exposed cells to $^{45}Ca^{2+}$ for 10 min after pre-incubation in absence or presence of inhibitors before washing with cold $La^{3+}$ solution. Cells were exposed to a $[^{45}Ca^{2+}]_{tracer}$ of ~0.12 nM in a 1.2 mM solution of $^{40}Ca^{2+}$ resulting in a $^{45}Ca^{2+}$:$^{40}Ca^{2+}$ ratio of $9.7\times10^6$. The initial rate of tracer influx is approximated by the slope or first derivative of the exponential uptake curve at time 0 (Fig. 1). This is equal to $Y_{max}$ (plateau) multiplied by the rate constant ($k$) giving an instantaneous influx rate of 161 cpm·min$^{-1}$, which was then converted to moles of $^{45}Ca^{2+}$-labeled $Ca^{2+}$ (see Appendix A). This conversion gives the instantaneous influx rate of $^{45}Ca^{2+}$, and the rate of $^{40}Ca^{2+}$ influx was assumed to be proportional to the ratio of $^{40}Ca^{2+}$:$^{45}Ca^{2+}$ in the tracer solution. We estimate the instantaneous influx of $Ca^{2+}$ into the SMC to be $5.9\times10^{14}$ $Ca^{2+}$·min$^{-1}$·well$^{-1}$. Each well contained an average of $4.0\times10^5$ cells, so cellular $Ca^{2+}$ influx was approximately $1.5\times10^9$ $Ca^{2+}$·cell$^{-1}$·min$^{-1}$. The average volume of 14 cells from three individual experiments was calculated to be 9.6±1.2 picolitres (volumes ranged from 3.6 to 15.8 picolitres). Therefore, we estimate the molar minute influx of $Ca^{2+}$ in our cultured smooth muscle cells to be on the order of $2.5\times10^{-4}$ M·min$^{-1}$, which corresponds to a whole cell current of approximately 7.5 pA.

### 3.3. Inhibition by gadolinium ion

Lanthanides have long been known to inhibit membrane $Ca^{2+}$ transport (Wallnofer et al., 1989), and it has been suggested that $Gd^{3+}$ can selectively inhibit SOC (Trebak et al., 2002). We investigated the concentration response relationship of $Gd^{3+}$ on inhibition of resting $Ca^{2+}$ influx (Fig. 4). The semi-log plot of this relation yields two well-separated inhibitory processes with Hill slopes for both of about −1. The first process accounts for 65–70% of total inhibition and has an $IC_{50}$ of 1 μM. The second process accounts for 30% of total inhibition with an $IC_{50}$ of 2 mM.

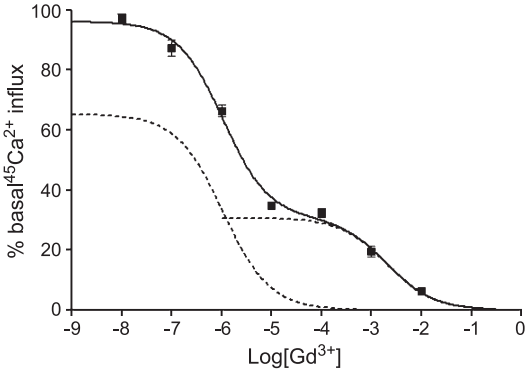


Fig. 4. Complex concentration-dependent inhibition of $^{45}Ca^{2+}$ uptake by gadolinium ion. Cells were incubated for 15 min in $GdCl_3$ then exposed to $^{45}Ca^{2+}$ tracer (0.4 μCi) for 10 min followed by removal of excess tracer as described above. The concentration–effect relationship was closely fit using a custom programmed bi-sigmoidal equation in GraphPad Prism (see Methods) where the initial values for iteration of the fit were set at: Hill $slopes_{1and2}$=−1, $pIC_{50\text{-}1}$=6 (visually estimated), $pIC_{50\text{-}2}$=3 (visually estimated), $Top_1$=70, $Top_2$=30, both bottoms=0). Two overlapping sigmoids were simulated from the resulting parameters (left dotted curve: $pIC_{50}$=6.0, Hill slope=−0.95, right dotted curve: $pIC_{50}$=−2.7, Hill slope=−0.92).

As illustrated below the larger more sensitive component is the result of inhibition of various $Ca^{2+}$ channels, which are also sensitive to more selective organic channel blockers. The smaller less sensitive component may be related to competition between $Gd^{3+}$ and $Ca^{2+}$ for negative binding sites on the plasma membrane (see Discussion).

### 3.4. Non-stimulated $Ca^{2+}$ entry through excitable $Ca^{2+}$ channels

We tested the hypothesis that part of the "resting" $Ca^{2+}$ influx was due to entry through the same types of $Ca^{2+}$ channels that support stimulated $Ca^{2+}$ entry. In other words we hypothesized that voltage-gated $Ca^{2+}$ channels, receptor-operated channels and store-operated channels display a background activity when the cells are not stimulated either electrically or chemically. Fig. 5 shows the inhibition of $^{45}Ca^{2+}$ uptake by maximally effective concentrations of nifedipine (10 μM; for L-type calcium channels), SKF 96365 (1-[*b*-[3-(4-Methoxyphenyl)propoxy]-4-methoxyphenethyl]-1H-imidazole) (50 μM; for L-type and receptor-operated channels) and 2-APB (75 μM; selective, but not specific for inisitol-1,4,5-trisphosphate ($IP_3$) receptor and some store-operated channels in addition to partial inhibitory effect on L-type channels).

From these results (Fig. 5) we deduced that distinct pathways contribute to resting $Ca^{2+}$ influx. Thus 45% of the resting $Ca^{2+}$ influx is mediated by voltage-gated $Ca^{2+}$ channels, which are completely blocked by nifedipine and SKF 96365 and are inhibited 50% by 75 μM 2-APB. 7% of the resting $Ca^{2+}$ influx is mediated by $Ca^{2+}$ channels exclusively blocked by SKF 96365 and, 23% of the resting $Ca^{2+}$ influx is mediated by channels blocked exclusively by 2-APB. This conclusion is dependent on the use of optimally blocking concentrations of the various agents as demonstrated for SKF 96365 and 2-APB in the presence

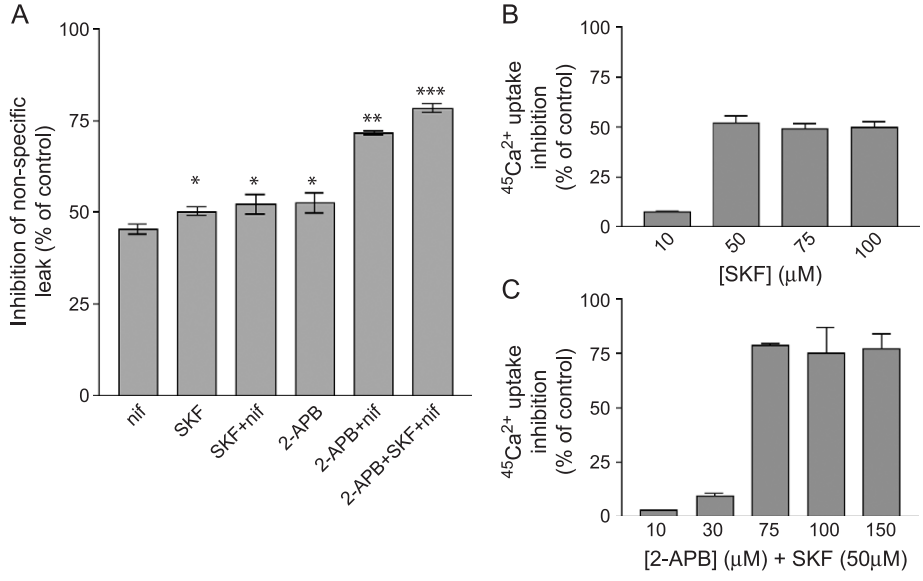


Fig. 5. Excitable calcium channels mediate calcium leak. (A) Investigation of known organic calcium channel blockers. Cells were pre-incubated with nifedipine (nif, 10 μM) or SKF 96365 (50 μM) for 15 min or 2-APB (75 μM) for 20 min before $^{45}Ca^{2+}$ tracer (0.4 μCi) was added to cells for a 10-min incubation period. Analysis of additivity: SKF 96365 inhibits $Ca_v1.2$ at this concentration, so $Ca_v1.2$ carries ~45% of the leak influx and channels exclusively sensitive to SKF 96365 carry ~7% of the influx. Channels uniquely sensitive to 2-APB carry ~23% of the resting $Ca^{2+}$ influx ($n$=6–15). (*=different from nif, **=different from SKF 96365, ***=different from 2-APB±SKF 96365. Determined by ANOVA ($p$<0.05) and pair-wise post-hoc analysis). (B) Concentration–response relationship for SKF 96365: This compound shows a very steep concentration–response relationship with a Hill slope ~3.0, and a maximal effective concentration of 50 μM ($n$=3). (C) Concentration–response relationship for 2-APB: The concentration–response relationship of 2-APB was determined in the presence of SKF 96365 (50 μM) to negate any cross-reactivity with SKF 96365-sensitive channels ($n$=3). Error bars represent standard error.

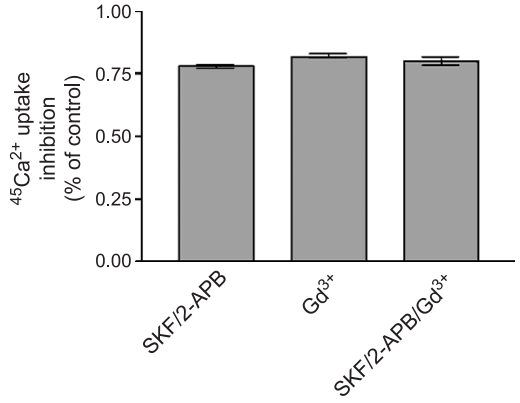


Fig. 6. A combination of SKF 96365 and 2-APB fully blocks resting influx through membrane channels. 100 μM $Gd^{3+}$ is an approximation of the maximal effective concentration for the first phase of $Gd^{3+}$-mediated inhibition of resting $^{45}Ca^{2+}$-influx, with little effect on the second phase of inhibition. SKF 96365 and 2-APB were used at their maximally effective concentrations. There is no significant difference between inhibition of resting $Ca^{2+}$ entry by organic inhibitors alone or in combination with $Gd^{3+}$ (100 μM), or by $Gd^{3+}$ (100 μM) alone (ANOVA with Bon Ferroni pair-wise comparison, $p$=0.07). Cells were pre-treated with inhibitors for 20 min before addition of $^{45}Ca^{2+}$ (0.4 μCi) for 10 min. Experiments represent the mean±standard error of eight replicates.

of nifedipine (10 μM) (Fig. 5B and C). Note that effective concentrations of 2-APB for inhibition of resting $Ca^{2+}$ influx are more consistent with those reported for inhibition of the $IP_3R$ ($IC_{50}$=42 μM) in the SR than SOC in the PM (reported to be 0.5 μM) (Su et al., 2003). We have previously shown 10 μM to be a maximally effective concentration of nifedipine (Perez-Vizcaino et al., 1993).

### 3.5. Comparison of organic $Ca^{2+}$ entry blockers with inorganic gadolinium

Due to the clear separation of the two inhibitory components of $Gd^{3+}$, we used a concentration of 100 μM $Gd^{3+}$ to completely block the more sensitive phase of $^{45}Ca^{2+}$ up-take, while leaving the less sensitive component essentially untouched (Fig. 4). This permitted us to address the question of whether there is a $Ca^{2+}$ channel that is uniquely and potently inhibited by $Gd^{3+}$. Three independent experiments showed that a combination of 75 μM 2-APB and 50 μM SKF 96365 exerts the same degree of inhibition (79.6±3.5%) as 100 μM $Gd^{3+}$ (83.7±1.2%). Furthermore, the $Ca^{2+}$ leak is not additively inhibited by organic and inorganic blockade (83.8±4.0%). This indicates that at concentrations below 100 μM, $Gd^{3+}$ blocks all three types of $Ca^{2+}$ channels: L-type $Ca^{2+}$ channels, "receptor-operated channels" and "store-operated channels". Moreover, the first phase of influx blockade by $Gd^{3+}$ occurs with a Hill Slope of ~1, which is commonly interpreted to indicate a single binding site. In this case we take this to indicate a lack of selectivity by $Gd^{3+}$ for any one of these channels.

### 3.6. Expression of candidate genes for channels responsible for non-stimulated $Ca^{2+}$ entry

The above experiments have helped to functionally characterize the channels contributing to the spontaneous background $Ca^{2+}$ leak, but do not identify the molecular identities involved with the exception of the L-type channel ($Ca_v1.2$), by virtue of the high degree of selectivity of nifedipine. Accordingly, RT-PCR detected expression of the L-type channel-specific α-subunit (data not shown). To date the most likely candidate molecules for receptor-operated and store-operated channels in mammalian cells are the cannonical transient receptor potential channels (TRPC channels) (Li et al., 2002; Nilius, 2003). Confluent cultured rat aortic smooth muscle cells expressed TrpC1, 4 and 6 mRNA, while homogenized rat brain, used as a positive control, revealed expression of TrpC1-7 mRNA (Fig. 7).

## 4. Discussion

We have analyzed basal $Ca^{2+}$ entry in non-stimulated, "resting" cells and have identified four pharmacologically distinct components: (1) voltage gated channels, (2) receptor operated channels, (3) store operated channels

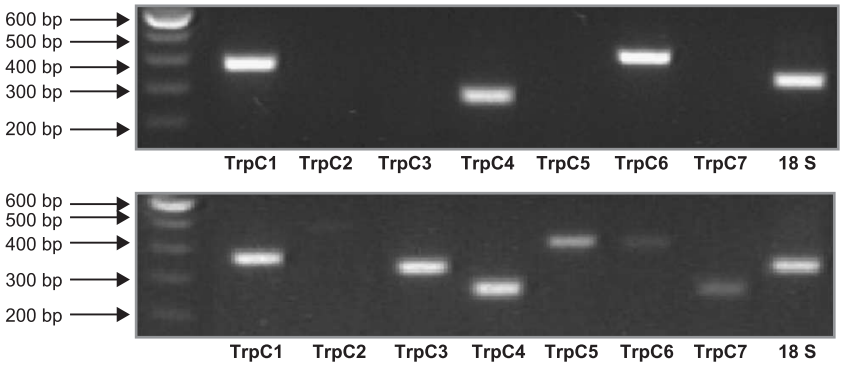


Fig. 7. TrpC mRNA expression profile in cultured rat aortic smc. Upper panel shows cDNA amplified by RT-PCR of total RNA isolated from confluent rat aortic smooth muscle cells at 7–9 days in culture. Lower panel shows a positive control for the probes using total RNA isolated from rat brain homogenate. All primers used amplified rat brain transcripts. (primer sequences in Table 1).

and (4) a smaller undefined component sensitive only to millimolar $Gd^{3+}$. This complements recent electrophysiological and molecular studies (Obejero-Paz et al., 1998; Nadler et al., 2001; Vandebrouck et al., 2002), and we illustrate here that basal $Ca^{2+}$ entry in smooth muscle cells is mainly mediated by a background open probability of electrically- and chemically-sensitive $Ca^{2+}$ permeable channels, which may be of similar molecular composition to "$Ca^{2+}$ leak channels" described in skeletal myotubes (Hopf et al., 1996; Vandebrouck et al., 2002). A large component, 70–80% of the total $Ca^{2+}$ influx, is carried by L-type $Ca^{2+}$ channels, receptor-operated channels and store-operated channels in proportions that will most probably vary markedly with cell type, culture conditions and specific TRPC expression profile. It is important to note that the cells used in this study do not necessarily reflect the properties of vascular smooth muscle under physiological conditions. For example the large basal entry through the L-type $Ca^{2+}$ channels may indicate that these cells are partly depolarized after reaching confluency (Knot et al., 1991). Indeed preliminary experiments indicated that nifedipine inhibited considerably less influx (about 25% of total influx) in younger, non-confluent cells (data not shown). However the most surprising finding was the large inhibition by 2-APB, which indicates the presence of open store-operated channels under resting conditions even though the sarcoplasmic reticulum contains ample stored $Ca^{2+}$ (Skutella and Ruegg, 1996; Szado et al., 2003). This finding is compatible with constant cycling of $Ca^{2+}$ between the sarcoplasmic reticulum and the extracellular space independent of changes in bulk cytoplasmic $[Ca^{2+}]_i$ (van Breemen et al., 1986). This illustrates that the plasmalemmal $Ca^{2+}$ leak is to some extent linked to the well-known sarcoplasmic reticulum $Ca^{2+}$ leak (Camello et al., 2002). The TRP family of proteins are likely candidates for the molecular constituents forming receptor-operated and store-operated channels, and these proteins can form non-selective cation channels (Nilius, 2003). Therefore, this may explain the resting activity of voltage-gated $Ca^{2+}$ channels, since opening of non-selective cation channels will tend to partially depolarize the cells (Zakharov et al., 1999).

In addition to the $Ca^{2+}$ leak carried by excitable $Ca^{2+}$ channels, a smaller component of 20–30% of basal $^{45}Ca^{2+}$ uptake is only inhibited by high concentrations of inorganic polyvalent cations such as $La^{3+}$ and $Gd^{3+}$. At present we do not know the mechanism for this uptake nor its physiological significance, but the concentrations of $La^{3+}$ or $Gd^{3+}$ required to inhibit this uptake are far greater than the $IC_{50}$'s reported for inhibition of activated $Ca^{2+}$ channels (Tiruppathi et al., 2002; Wallnofer et al., 1989). Close inspection of the uptake kinetics reveals a small component of uptake with a $t_{1/2}$ of approximately 7 s, which is faster than would be energetically favourable for channel permeation. In addition, the magnitude of this rapid component was dramatically reduced after enhancing the stringency of the $^{45}Ca^{2+}$ washout protocol (Fig. 1). This suggests the presence of a protected extracellular $Ca^{2+}$ pool that is not readily displaced from its binding sites such as described Darby et al. (2000). If extracellular binding sites are involved, the 15-min $Gd^{3+}$ pre-incubation used to create the $Gd^{3+}$ concentration–effect curve may effectively act as a blocking step, or alternatively may block internalization of the tracer. However, this conclusion remains speculative.

It is particularly interesting that the $Ca^{2+}$ channels contributing to basal $Ca^{2+}$ entry that are sensitive to low micromolar concentrations of lanthanides appear to be the same channels already functionally identified in smooth muscle: voltage-gated, receptor-operated and store-operated channels. Other candidates for channels contributing to basal $Ca^{2+}$ entry are stretch-activated channels and the "leak channels" recorded in skeletal muscle (Hopf et al., 1996). Setoguchi et al. showed that stretch-activated channels are inhibited by $Gd^{3+}$ with an $IC_{50}$ of 14 μM and are completely blocked by 100 μM $Gd^{3+}$(Setoguchi et al., 1997). We cannot confirm or dispute a role for stretch-active channels in these cultured cells, but the lack of additivity of $Gd^{3+}$ on top of SKF 96365 and 2-APB would imply that if stretch-activated channels are expressed and are contributing to the $Ca^{2+}$ leak then they are also sensitive to these organic compounds. The skeletal muscle "leak channels," which may also be stretch-sensitive, are activated by nifedipine and inhibited by two unique dihydropyridines, AN-1043 (dimethyl 2,6-dimethyl-4-(4-bromophenyl)-1,4-dihydropyridine-3,5- dicarboxylate) and AN-406 (dimethyl 2,6-dimethyl-4-(4-trifluoromethyl-phenyl)-1,4-dihydropyridine-3,5-dicarboxylate) (Alderton and Steinhardt, 2000; Hopf et al., 1996). However there is no evidence to date as to their sensitivity to SKF 96365, 2-APB or $Gd^{3+}$. On the other hand Obejero-Paz et al. (1998) have electrophysiologically characterized two distinct "leak channels" in A7r5 cultured smooth muscle cells. One channel was divalent cation-selective (6pS), and the other was a relatively non-selective channel (17 pS), and these channels are inhibited by 50 μM $Gd^{3+}$. Moreover, the 17 pS channel shares some electrophysiological characteristics with the skeletal muscle leak channels and the drosphila TRPC-L channel.

Of the known excitable $Ca^{2+}$ channels, current literature overwhelmingly points towards the TRPC channels as mediating the phenomena of receptor-activated and store-activated calcium influx. Generally, TRPC6 and 7 are thought to be activated by diacylglycerol (Gamberucci et al., 1994; Jung et al., 2002; Vennekens et al., 2002), while different reports show TRPC1, 3, 4 and 5 to be activated by both receptor-activation or store-depletion depending on the experimental conditions (Li et al., 2002; Nilius, 2003; Obukhov and Nowycky, 2002; Plant and Schaefer, 2003). This variable activation most likely reflects extensive species- and tissue-specific signaling, which makes it difficult to definitively label these

channels as receptor-operated or store-operated channels (Nilius, 2003). More importantly however, Gailly's group showed TRPC1 and 4 to be constitutively active in A7r5 smooth muscle cells (Vandebrouck et al., 2002), and TRPC7 has been implicated as contributing to basal plasmalemmal permeability to divalent cations by virtue of its activation by intracellular Mg·ATP and Mg·GTP (Nadler et al., 2001). On the other hand Vanderbrouke et al. found that TRPC6 was not constitutively active, which is consistent with its specific roll as a receptor-operated channel. TRPC1 is linked to the type-2 $IP_3$ receptor in some cells, which might confer sensitivity to the release of intracellular $Ca2^+$ stores (Ma et al., 2000) Further more, it is important to note that heteromeric TRPC channels often exhibit radically different characteristics from those reported for the respective homomeric channels. (Goel et al., 2002). Thus since the cultured rat aortic smooth muscle cells in our study expressed TRPC1, 4 and 6, we propose that these cells express at least two forms of store-sensitive cation channel (TRPC1 and TRPC4) and at least one of type of channel that is selectively regulated by receptor activation (TRPC6).

Although the pharmacology of TRPC channel modulation is still in its infancy, initial reports indicate that TRPC1 and 6 are inhibited by $La^{3+}$ (2–50μM) and are also sensitive to SKF 96365, which incidentally has been shown to inhibit TRPC3 (Boulay et al., 1997; Zhu et al., 1998). Several reports have shown 2-APB to inhibit store-operated $Ca^{2+}$ entry, presumably carried by TRPC channels (Bootman et al., 2002). To be specific 2-APB can inhibit TRPC3 (Trebak et al., 2002, 2003). In rabbit inferior vena cava, which expresses only TrpC1 mRNA, SKF 96365, but not 2-APB, inhibited store refilling (Lee et al., 2002). Thus we hypothesize that the portion of the $Ca^{2+}$ leak that is selectively blocked by 2-APB is carried by TRPC4. However, the potency that we observed for 2-APB's action on $Ca^{2+}$ leak inhibition is more consistent with inhibition of $IP_3$ receptors than direct inhibition of a plasmalemmal channel (Su et al., 2003). This implies: (1) that the $IP_3$ receptor channels have a basal open probablility, which could offer one pathway for the sarco/endoplasmic reticulum $Ca^{2+}$ leak, and (2) that the resting $Ca^{2+}$ leak from the sarcoplasmic reticulum is required and sufficient for the activation of TRPC4. This activity of 2-APB is in addition to partial inhibition of $Ca_v1.2$ at the concentrations used, which as mentioned above may be an indirect effect. The fact that TRPC6 was shown to not be active in resting A7r5 smooth muscle cells (Vandebrouck et al., 2002), further indicates that 2-APB was selectively inhibiting TRPC4 in our cultured smooth muscle cells. By corollary, this would infer that the portion of the $Ca^{2+}$ leak that was specifically blocked by SKF 96365 may have been purely mediated by TRPC1. This would be consistent with the report from Scarpa's group that only two single channel currents were active in the A7r5 cell $Ca^{2+}$ leak (Obejero-Paz et al., 1998).

Having characterized the nature of the calcium leak in the RASMC, we must question the physiological significance of 2.4 femtomoles of $Ca^{2+}$ permeating the cell membrane per minute. Is this influx sufficient to maintain intracellular calcium stores? In relation to cell volume, this corresponds to a turnover of 250 μM per minute, which at first seems excessive given a resting $[Ca^{2+}]_i$ of ~100 nM. Yet for comparison, Ganitkevich calculated a single episode of $Ca^{2+}$ release from the endoplasmic reticulum to be 680 attomoles of $Ca^{2+}$ (Ganitkevich, 1996). Thus, resting $Ca^{2+}$ influx could provide sufficient $Ca^{2+}$ to compensate for spontaneous $Ca^{2+}$ sparks and puffs in resting cells, and in fact may be stimulated by these quantal release events from sarcoplasmic reticulum $Ca^{2+}$ On the other hand, this rate of resting calcium leak is equivalent to an inward current of ~7.5 pA, compared to a single open L-type channel carring 0.3 pA (Gollasch et al., 1992), and this magnitude of unstimulated influx is amenable to the concept of "leaky" or "flickering" excitable channels, being equivalent to 250 channels with a basal open probability of 0.1.

Moreover, it is important to consider how these findings in cultured cells relate to intact vascular smooth muscle. Removal of extracellular $Ca^{2+}$ depletes intracellular $Ca^{2+}$ stores (Nazer and van Breemen, 1998), which implies that basal $Ca^{2+}$ influx is required to maintain the resting $Ca^{2+}$ concentration in the sarcoplasmic reticulum of intact vascular smooth muscle. The compounds used herein to inhibit the $Ca^{2+}$ leak are also known to inhibit vascular contraction, thus it is of immediate interest to assess whether this is in part due to a loss of reticular $Ca^{2+}$ stores in a manner analogous to removing extracellular $Ca^{2+}$.

## Acknowledgements

We would like to thank Mr. Eric Lin for his generous assistance with image analysis. We would like to thank the Swiss National Science Foundation (grant Nr. 31-68315.02), the British Columbia Children's Hospital Foundation and the Canadian Heart and Stroke Foundation for project funding support and the Foundation Herbette of the University of Lausanne, the Michael Smith Foundation for Health Research and the National Science and Engineering Research Council for their generous personnel and training support. We would also like to thank Dr. Tullio Pozzan for generously providing the SNAP-GFP plasmid.

## Appendix A. Converting tracer uptake to $^{40}Ca^{2+}$ influx

$[^{45}Ca^{2+}]_{stock}$: Stock tracer solution was diluted 1000-fold, and the activity in six 20-μl alliquots was counted giving an average diluted activity of $3.90\times10^4$ cpm. Accordingly, the stock contained $1.95\times10^9$ cpm/ml. Given

a half life of 163 days and 90% counting efficiency, the concentration of $^{45}Ca^{2+}$ ion required to give this activity is $7.31\times10^{14}$ ions/ml based on simple exponential decay. This is equivalent to $1.22\times10^{-6}$ mol/l, and gives a conversion factor of $3.76\times10^{5}$ $^{45}Ca^{2+}$/cpm. This values was then corrected to account for decay of the stock from the time when the uptake measurements were performed (30 days prior) to give a $[^{45}Ca^{2+}]_{stock}$ of $1.37\times10^{-6}$ M.

*$[^{45}Ca^{2+}]_{on\ cells}$ and $^{40}Ca^{2+}$-to-$^{45}Ca^{2+}$ ratio:* Upon addition of tracer to the experimental wells, the $[^{45}Ca^{2+}]_{stock}$ had been diluted 11 000-fold giving a $[^{45}Ca^{2+}]_{on\ cells}$ of $1.24\times10^{-10}$ M. The physiological saline solution used contained nominally 1.2 mM $Ca^{2+}$ giving a $^{40}Ca^{2+}$-to-$^{45}Ca^{2+}$ ratio of $9.68\times10^{6}$.

*Basal $Ca^{2+}$ permeability*: the instantaneous $^{45}Ca^{2}$ uptake rate of 161 cpm $\cdot$ $min^{-1}$ was calculated as the first derivative of the influx kinetics curve at $t$=0, which is equivalent to a rate constant multiplied by the curve plateau ($k$=0.084, $Y_{max}$=1920). Converting cpm to $^{40}Ca^{2+}$ ions gives $5.86\times10^{14}$ $^{40}Ca^{2+}\cdot min^{-1}\cdot well^{-1}$. Given that each well contained $4.04\times10^{5}$cells on average, the basal cellular influx of $Ca^{2+}$ was $1.45\times10^{9}$ $Ca^{2+}\cdot min^{-1}$.

## References


Alderton, J.M., Steinhardt, R.A., 2000. Calcium influx through calcium leak channels is responsible for the elevated levels of calcium-dependent proteolysis in dystrophic myotubes. J. Biol. Chem. 275, 9452–9460.

Bootman, M.D., Collins, T.J., Mackenzie, L., Roderick, H.L., Berridge, M.J., Peppiatt, C.M., 2002. 2-aminoethoxydiphenyl borate (2-APB) is a reliable blocker of store-operated Ca2+ entry but an inconsistent inhibitor of InsP3-induced Ca2+ release. FASEB J. 16, 1145–1150.

Boulay, G., Zhu, X., Peyton, M., Jiang, M., Hurst, R., Stefani, E., Birnbaumer, L., 1997. Cloning and expression of a novel mammalian homolog of drosophila transient receptor potential (Trp) involved in calcium entry secondary to activation of receptors coupled by the Gq class of G protein. J. Biol. Chem. 272, 29672–29680.

Busselberg, D., Platt, B., Michael, D., Carpenter, D.O., Haas, H.L., 1994. Mammalian voltage-activated calcium channel currents are blocked by Pb2+, Zn2+, and Al3+. J. Neurophysiol. 71, 1491–1497.

Camello, C., Lomax, R., Petersen, O.H., Tepikin, A.V., 2002. Calcium leak from intracellular stores—the enigma of calcium signalling. Cell Calcium 32, 355–361.

Casteels, R., Droogmans, G., 1981. Exchange characteristics of the noradrenaline-sensitive calcium store in vascular smooth muscle cells or rabbit ear artery. J. Physiol. 317, 263–279.

Darby, P.J., Kwan, C.Y., Daniel, E.E., 2000. Caveolae from canine airway smooth muscle contain the necessary components for a role in Ca(2+) handling. Am. J. Physiol., Lung Cell Mol. Physiol. 279, L1226–L1235.

Deth, R., van Breemen, C., 1974. Relative contributions of Ca2+ influx and cellular Ca2+ release during drug induced activation of the rabbit aorta. Pflugers Arch. 348, 13–22.

Fayazi, A.H., Lapidot, S.A., Huang, B.K., Tucker, R.W., Phair, R.D., 1996. Resolution of the basal plasma membrane calcium flux in vascular smooth muscle cells. Am. J. Physiol., Heart. Circ. Physiol. 270, H1972–H1978.

Gamberucci, A., Innocenti, B., Fulceri, R., Banhegyi, G., Giunti, R., Pozzan, T., Benedetti, A., 1994. Modulation of Ca2+ influx dependent on store depletion by intracellular adenine-guanine nucleotide levels. J. Biol. Chem. 269, 23597–23602.

Ganitkevich, V.Y., 1996. The amount of acetylcholine mobilisable Ca2+ in single smooth muscle cells measured with the exogenous cytoplasmic Ca2+ buffer, Indo-1. Cell Calcium 20, 483–492.

Goel, M., Sinkins, W.G., Schilling, W.P., 2002. Selective association of TRPC channel subunits in rat brain synaptosomes. J. Biol. Chem. 277, 48303–48310.

Gollasch, M., Hescheler, J., Quayle, J.M., Patlak, J.B., Nelson, M.T., 1992. Single calcium channel currents of arterial smooth muscle at physiological calcium concentrations. Am. J. Physiol. 263, C948–C952.

Grasso, P., Santa-Coloma, T.A., Reichert Jr., L.E., 1992. Correlation of follicle-stimulating hormone (FSH)-receptor complex internalization with the sustained phase of FSH-induced calcium uptake by cultured rat Sertoli cells. Endocrinology 131, 2622–2628.

Hopf, F.W., Reddy, P., Hong, J., Steinhardt, R.A., 1996. A capacitative calcium current in cultured skeletal muscle cells is mediated by the calcium-specific leak channel and inhibited by dihydropyridine compounds. J. Biol. Chem. 271, 22358–22367.

Jung, S., Strotmann, R., Schultz, G., Plant, T.D., 2002. TRPC6 is a candidate channel involved in receptor-stimulated cation currents in A7r5 smooth muscle cells. Am. J. Physiol., Cell Physiol. 282, C347–C359.

Knot, H.J., de Ree, M.M., Gahwiler, B.H., Ruegg, U.T., 1991. Modulation of electrical activity and of intracellular calcium oscillations of smooth muscle cells by calcium antagonists, agonists, and vasopressin. J. Cardiovasc. Pharmacol. 18 (Suppl. 10), S7–S14.

Lee, C.H., Rahimian, R., Szado, T., Sandhu, J., Poburko, D., Behra, T., Chan, L., van Breemen, C., 2002. Sequential opening of IP(3)-sensitive Ca(2+) channels and SOC during alpha-adrenergic activation of rabbit vena cava. Am. J. Physiol., Heart Circ. Physiol. 282, H1768–H1777.

Li, S.W., Westwick, J., Poll, C.T., 2002. Receptor-operated Ca2+ influx channels in leukocytes: a therapeutic target? Trends Pharmacol. Sci. 23, 63–70.

Lo Russo, A., Passaquin, A.C., Andre, P., Skutella, M., Ruegg, U.T., 1996. Effect of cyclosporin A and analogues on cytosolic calcium and vasoconstriction: possible lack of relationship to immunosuppressive activity. Br. J. Pharmacol. 118, 885–892.

Ma, H.T., Patterson, R.L., van Rossum, D.B., Birnbaumer, L., Mikoshiba, K., Gill, D.L., 2000. Requirement of the inositol trisphosphate receptor for activation of store-operated Ca2+ channels. Science 287, 1647–1651.

Marsault, R., Murgia, M., Pozzan, T., Rizzuto, R., 1997. Domains of high Ca2+ beneath the plasma membrane of living A7r5 cells. EMBO J. 16, 1575–1581.

McDaniel, S.S., Platoshyn, O., Wang, J., Yu, Y., Sweeney, M., Krick, S., Rubin, L.J., Yuan, J.X., 2001. Capacitative Ca(2+) entry in agonist-induced pulmonary vasoconstriction. Am. J. Physiol., Lung Cell Mol. Physiol. 280, L870–L880.

Nadler, M.J., Hermosura, M.C., Inabe, K., Perraud, A.L., Zhu, Q., Stokes, A.J., Kurosaki, T., Kinet, J.P., Penner, R., Scharenberg, A.M., Fleig, A., 2001. LTRPC7 is a Mg.ATP-regulated divalent cation channel required for cell viability. Nature 411, 590–595.

Nazer, M.A., van Breemen, C., 1998. Functional linkage of Na(+)-Ca2+ exchange and sarcoplasmic reticulum Ca2+ release mediates Ca2+ cycling in vascular smooth muscle. Cell Calcium 24, 275–283.

Nilius, B., 2003. From TRPs to SOCs, CCEs, and CRACs: consensus and controversies. Cell Calcium 33, 293–298.

Nowycky, M.C., Fox, A.P., Tsien, R.W., 1985. Long-opening mode of gating of neuronal calcium channels and its promotion by the dihydropyridine calcium agonist Bay K 8644. Proc. Natl. Acad. Sci. U. S. A. 82, 2178–2182.

Obejero-Paz, C.A., Jones, S.W., Scarpa, A., 1998. Multiple channels mediate calcium leakage in the A7r5 smooth muscle- derived cell line. Biophys. J. 75, 1271–1286.

Obukhov, A.G., Nowycky, M.C., 2002. TRPC4 can be activated by G-protein-coupled receptors and provides sufficient Ca(2+) to trigger exocytosis in neuroendocrine cells. J. Biol. Chem. 277, 16172–16178.

Perez-Vizcaino, F., Tamargo, J., Hof, R.P., Ruegg, U.T., 1993. Vascular selectivity of seven prototype calcium antagonists: a study at the single cell level. J. Cardiovasc. Pharmacol. 22, 768–775.

Plant, T.D., Schaefer, M., 2003. TRPC4 and TRPC5: receptor-operated $Ca^{2+}$-permeable nonselective cation channels. Cell Calcium 33, 441–450.

Rudolf, R., Mongillo, M., Rizzuto, R., Pozzan, T., 2003. Looking forward to seeing calcium. Nat. Rev., Mol. Cell Biol. 4, 579–586.

Setoguchi, M., Ohya, Y., Abe, I., Fujishima, M., 1997. Stretch-activated whole-cell currents in smooth muscle cells from mesenteric resistance artery of guinea-pig. J. Physiol. 501, 343–353.

Skutella, M., Ruegg, U.T., 1996. Increase of empty pool-activated Ca2+ influx using an intracellular Ca2+ chelating agent. Biochem. Biophys. Res. Commun. 218, 837–841.

Su, Z., Barker, D.S., Csutora, P., Chang, T., Shoemaker, R.L., Marchase, R.B., Blalock, J.E., 2003. Regulation of Ca2+ release-activated Ca2+ channels by INAD and Ca2+ influx factor. Am. J. Physiol., Cell Physiol. 284, C497–C505.

Szado, T., Kuo, K.H., Bernard-Helary, K., Poburko, D., Lee, C.H., Seow, C., Ruegg, U.T., van Breemen, C., 2003. Agonist-induced mitochondrial Ca2+ transients in smooth muscle. FASEB J. 17, 28–37.

Tiruppathi, C., Freichel, M., Vogel, S.M., Paria, B.C., Mehta, D., Flockerzi, V., Malik, A.B., 2002. Impairment of store-operated Ca2+ entry in TRPC4(−/−) mice interferes with increase in lung microvascular permeability. Circ. Res. 91, 70–76.

Trebak, M., Bird, G.S., McKay, R.R., Putney Jr., J.W., 2002. Comparison of human TRPC3 channels in receptor-activated and store- operated modes. Differential sensitivity to channel blockers suggests fundamental differences in channel composition. J. Biol. Chem. 277, 21617–21623.

Trebak, M., Vazquez, G., Bird, G.S., Putney Jr., J.W., 2003. The TRPC3/6/7 subfamily of cation channels. Cell Calcium 33, 451–461.

van Breemen, C., 1968. Permselectivity of a porous phospholipid-cholesterol artificial membrane. Calcium and lanthanum effects. Biochem. Biophys. Res. Commun. 32, 977–983.

Van Breemen, D., van Breemen, C., 1969. Calcium exchange diffusion in a porous phospholipid ion-exchange membrane. Nature 223, 898–900.

van Breemen, C., Farinas, B.R., Casteels, R., Gerba, P., Wuytack, F., Deth, R., 1973. Factors controlling cytoplasmic Ca2+ concentration. Philos. Trans. R. Soc. Lond., B Biol. Sci. 265, 57–71.

van Breemen, C., Cauvin, C., Johns, A., Leijten, P., Yamamoto, H., 1986. Ca2+ regulation of vascular smooth muscle. Fed. Proc. 45, 2746–2751.

Vandebrouck, C., Martin, D., Schoor, M.C.-V., Debaix, H., Gailly, P., 2002. Involvement of TRPC in the abnormal calcium influx observed in dystrophic (mdx) mouse skeletal muscle fibers. J. Cell Biol. 158, 1089.

Vennekens, R., Voets, T., Bindels, R.J.M., Droogmans, G., Nilius, B., 2002. Current understanding of mammalian TRP homologues. Cell Calcium 31, 253–264.

Walker, R.L., Hume, J.R., Horowitz, B., 2001. Differential expression and alternative splicing of TRP channel genes in smooth muscles. Am. J. Physiol., Cell Physiol. 280, C1184–C1192.

Wallnofer, A., Cauvin, C., Lategan, T.W., Ruegg, U.T., 1989. Differential blockade of ago. Am. J. Physiol. 257, C607–C611.

Zakharov, S.I., Mongayt, D.A., Cohen, R.A., Bolotina, V.M., 1999. Monovalent cation and L-type Ca2+ channels participate in calcium paradox-like phenomenon in rabbit aortic smooth muscle cells. J. Physiol. 514 (Pt 1), 71–81.

Zhu, X., Jiang, M., Birnbaumer, L., 1998. Receptor-activated Ca2+ influx via human Trp3 stably expressed in human embryonic kidney (HEK)293 cells. Evidence for a non-capacitative Ca2+ entry. J. Biol. Chem. 273, 133–142.